

This is a repository copy of *Abnormal visual gain control and excitotoxicity in early-onset Parkinson's disease Drosophila models*.

White Rose Research Online URL for this paper:

<https://eprints.whiterose.ac.uk/125459/>

Version: Accepted Version

Article:

Himmelberg, Marc Mason orcid.org/0000-0001-9133-7984, West, Ryan John Hatcher, Elliott, Christopher John Hazell orcid.org/0000-0002-5805-3645 et al. (1 more author) (2018) Abnormal visual gain control and excitotoxicity in early-onset Parkinson's disease *Drosophila* models. *Journal of Neurophysiology*. jn.00681.2017. pp. 957-970. ISSN 0022-3077

<https://doi.org/10.1152/jn.00681.2017>

Reuse

Items deposited in White Rose Research Online are protected by copyright, with all rights reserved unless indicated otherwise. They may be downloaded and/or printed for private study, or other acts as permitted by national copyright laws. The publisher or other rights holders may allow further reproduction and re-use of the full text version. This is indicated by the licence information on the White Rose Research Online record for the item.

Takedown

If you consider content in White Rose Research Online to be in breach of UK law, please notify us by emailing eprints@whiterose.ac.uk including the URL of the record and the reason for the withdrawal request.

1 **Abnormal visual gain control and excitotoxicity in early-onset Parkinson's**
2 **disease *Drosophila* models**

3

4 Marc M. Himmelberg^{1*}, Ryan J.H. West², Christopher J.H. Elliott², and Alex R.
5 Wade¹

6

7 ¹ Department of Psychology, The University of York, York

8 ² Department of Biology, The University of York, York

9 *Corresponding author

10

11 Abbreviated title/running head: GAIN CONTROL AND EXCITOTOXICITY IN PD
12 MODELS

13

14 Address for correspondence: M.M. Himmelberg, Department of Psychology,
15 University of York, York, United Kingdom, YO10 4DD (email:
16 marchimmelberg@gmail.com)

17

18

19

20

21

22

23

24

25

26

Abstract

27 The excitotoxic theory of Parkinson's disease (PD) hypothesises that a
28 pathophysiological degeneration of dopaminergic neurons stems from neural
29 hyperactivity at early stages of disease, leading to mitochondrial stress and cell
30 death. Recent research has harnessed the visual system of *Drosophila* PD models
31 to probe this hypothesis. Here, we investigate whether abnormal visual sensitivity
32 and excitotoxicity occur in early-onset PD (EOPD) *Drosophila* models *DJ-1* ^{$\Delta 72$} , *DJ1-*
33 *$\beta^{\Delta 93}$* , and *PINK1*⁵. We used an electroretinogram to record steady state visually
34 evoked potentials driven by temporal contrast stimuli. At 1 day of age, all EOPD
35 mutants had a twofold increase in response amplitudes when compared to *w*⁻
36 controls. Further, we found that excitotoxicity occurs in older EOPD models after
37 increased neural activity is triggered by visual stimulation. In an additional analysis,
38 we used a linear discriminant analysis to test whether there were subtle variations in
39 neural gain control that could be used to classify *Drosophila* into their correct age
40 and genotype. The discriminant analysis was highly accurate, classifying *Drosophila*
41 into their correct genotypic class at all age groups at 50-70% accuracy (20% chance
42 baseline). Differences in cellular processes link to subtle alterations in neural
43 network operation in young flies – all of which lead to the same pathogenic outcome.
44 Our data are the first to quantify abnormal gain control and excitotoxicity in EOPD
45 *Drosophila* mutants. We conclude that EOPD mutations may be linked to more
46 sensitive neuronal signalling in prodromal animals that may cause the expression of
47 PD symptomologies later in life.

48

49 **New and Noteworthy:** SSVEP response amplitudes to multivariate temporal
50 contrast stimuli were recorded in early-onset PD *Drosophila* models. Our data

51 indicate that abnormal gain control and a subsequent visual loss occur in these PD
52 mutants, supporting a broader excitotoxicity hypothesis in genetic PD. Further, linear
53 discriminant analysis could accurately classify *Drosophila* into their correct genotype
54 at different ages throughout their lifespan. Our results suggest increased neural
55 signalling in prodromal PD patients.

56

57 **Keywords:** Parkinson's disease, Gain Control, Excitotoxicity, SSVEPs, *Drosophila*,
58 Linear Discriminant Analysis

59

60

61

62

63

64

65

66

67

68

69

70

71

72

73

74

75

76

Introduction

77

78

79

80

81

82

83

84

85

86

87

88

89

90

91

92

93

94

95

96

97

98

99

100

Parkinson's Disease (PD) is the second most common progressive neurodegenerative disorder, affecting ~0.2-3% of the population, with an increased prevalence in those aged over 50 (Clarke, 2007; de Rijk et al., 1997). PD is thought to stem from the pathophysiologic degeneration and subsequent loss of dopaminergic neurons within the pars compacta of the substantia nigra, a basal ganglia structure that plays a key role in movement (Clarke, 2007). It is hypothesised that neuronal death in PD is caused by an excitotoxic mechanism, in which neuronal hyperactivity leads to neurodegeneration. Neuronal hyperactivity causes an increase in demand for ATP from mitochondria, leading to oxidative stress and eventual neuronal death (Beal et al., 1993; Surmeier, Obeso, & Halliday, 2017). In both mammals and invertebrates, neuronal responses are regulated by a tightly-linked network of excitatory and inhibitory gain control mechanisms that, collectively, we refer to as 'normalization' (Carandini & Heeger, 1994; Carandini, Heeger, & Movshon, 1997; Carandini & Heeger, 2011; Single, Haag, & Borst, 1997). Normalization mechanisms can be measured across the animal kingdom using a range of methods, including steady state visually evoked potential (SSVEP) recordings, a sensitive technique commonly used to measure the amplitude of neural population responses to periodic flickering stimuli (Busse, Wade, & Carandini, 2009; Norcia, Appelbaum, Ales, Cottareau, & Rossion, 2015; Regan, 1966; Tyler, Apkarian, & Nakayama, 1978).

In *Drosophila*, SSVEP recordings are collected from the surface of the eye and can be made in both healthy and PD mutant *Drosophila* (Afsari et al., 2014; West, Elliott, & Wade, 2015a). Previously we have shown that young flies carrying

101 the late-onset gain-of-function PD mutation *LRRK2-G2019S* showed *increased*
102 visual contrast sensitivity to full field flicker stimuli, reflecting a failure in regulation of
103 neural activity (i.e. abnormal gain control or normalization) at one day of age (Afsari
104 et al., 2014). This regulatory failure is followed by a decline in visual function over
105 time, with physiological and anatomical degeneration in older *LRRK2-G2019S*
106 *Drosophila* (Hindle et al., 2013; Mortiboys et al., 2015).

107

108 Feeding *LRRK2-G2019S Drosophila* with BMPPB-32, a kinase inhibitor
109 specifically targeted at *LRRK2*, restored normal contrast sensitivity at both 1 and 14
110 days of age, indicating that both the early neuronal hypersensitivity and the
111 subsequent neurodegeneration are due to abnormal kinase domain activity (Afsari et
112 al., 2014). Vision loss was accelerated by increasing neural activity via photic
113 stimulation of the *Drosophila* visual system using flashing LED lights. Together,
114 these findings support an excitotoxicity theory of the *LRRK2-G2019S* form of PD.
115 This excitotoxicity theory of PD has also found support in rodent models of the
116 *G2019S* mutation (Longo, Russo, Shimshek, Greggio, & Morari, 2014; Matikainen-
117 Ankney et al., 2016; Ponzio et al., 2017; Sloan et al., 2016; Volta et al., 2017).

118

119 We have previously demonstrated that linear discriminant analysis (LDA) is a
120 useful tool in the analysis of SSVEP data obtained from *Drosophila* (West, Elliott, &
121 Wade, 2015b). Here, our findings indicated differences in SSVEP amplitude both
122 between and within wild type flies and EOPD mutants, in response to spatiotemporal
123 patterns. These differences had enough statistical regularity for LDA to accurately
124 discriminate between genotypes. When compared to wild-type controls, qualitative
125 observations indicated an elevation in SSVEP response in 1 day old EOPD flies.

126 Although LDA has diagnostic utility, it does not allow for the quantification of
127 directional differences in such responses. Having established this method, we now
128 seek to expand upon this and investigate abnormal gain control and excitotoxicity in
129 EOPD models.

130

131 Is excitotoxicity a general feature of all *Drosophila* PD mutants? If so, it would
132 suggest that rather than being an epiphenomenon of some metabolic dysfunction
133 that causes PD, the excitotoxicity itself is central to the disease. In the current paper,
134 we use SSVEP techniques combined with principal components analysis, general
135 linear modelling, and multivariate classification analysis, to investigate abnormal gain
136 control and excitotoxicity in EOPD *Drosophila* models. We hypothesised that
137 abnormal gain control would occur in young *Drosophila* carrying EOPD mutations
138 due to disease related changes in retinal dopaminergic neurons, reflected by
139 increased SSVEP amplitudes in 1 day old EOPD *Drosophila* mutants. We also
140 hypothesised that abnormal gain control would cause an excitotoxic cascade in older
141 EOPD *Drosophila*. Consequently, we expected to observe a decrease in SSVEP
142 amplitudes at later ages. Finally, we wondered if all mutations affected neuronal gain
143 control in the same manner or if there were subtle mechanistic variations that could
144 be used to differentiate the genotypes. To address this, we used linear discriminant
145 analysis based on SSVEP responses to a range of temporal modulation rates and
146 contrast levels to attempt to classify flies into their correct genotypic class at different
147 points throughout their lifespan. The greater the differences in the gain control
148 profiles across genotypes, the greater the accuracy we expected from this
149 classification.

150

151 We found that SSVEP response amplitudes to spatial stimuli are significantly
152 increased in EOPD mutants at 1 day of age – indicating that neuronal gain control is
153 abnormal in these animals. Generating additional neuronal stress by exposing flies
154 to randomly pulsating light for 7 days resulted in a profound loss of vision in all PD
155 mutants, supporting the excitotoxicity model of PD. Finally, there are robust
156 differences between the temporal contrast response profiles of the different PD
157 mutants which allow our multivariate classification algorithms to classify flies into
158 their respective genotypes at well above chance levels throughout their lifespan.

159

160

Materials and Methods

161 *Drosophila stocks and maintenance*

162 *Drosophila* were raised in a 12hr:12hr light:dark (LD) cycle at 25° on standard
163 food consisting of agar (1% w/v), cornmeal (3.9%), yeast (3.7%), and sucrose
164 (9.4%). All flies were outcrossed and stabilised where appropriate to remove any
165 naturally occurring mutations. Three EOPD mutations (*DJ-1* $\alpha^{\Delta 72}$, *DJ1- $\beta^{\Delta 93}$* , and
166 *PINK1*⁵), one knockout of the fly *LRRK2* homologue (*dLRRK*^{ex1}) and one wild-type
167 control genotype (*w*¹¹¹⁸, herein *w*⁻) were deployed. *w*⁻ strains were gifted by Sean
168 Sweeney. *PINK1*⁵ and *dLRRK*^{ex1} strains were obtained from the Bloomington
169 *Drosophila* Stock Centre (Indiana, USA), whilst *DJ-1* $\alpha^{\Delta 72}$ and *DJ1- $\beta^{\Delta 93}$* strains were
170 kind gifts from Alex Whitworth. Male flies all had white eyes, and were tested at 1, 7,
171 14, 21, and 28 days post eclosion.

172

173 *Preparation of Drosophila for Testing*

174 Male flies were collected within 8 hours of eclosion and transferred to a new
175 vial of standard food that additionally contained nipagin (0.1% w/v). Flies were

176 maintained in these vials and transferred to fresh food weekly. Flies were kept in a
177 12hr:12hr LD cycle at 25°C until they had reached appropriate age for testing.

178

179 *Photic stress*

180 To explore as to whether an increase in neural demand resulted in a
181 decrease in SSVEP amplitudes, all *Drosophila* genotypes were exposed to a photic
182 stressor condition (Afsari et al., 2014; Hindle et al., 2013). Male flies were collected
183 within 8 hours of eclosion and transferred to a new vial of standard food containing
184 nipagin. These flies were maintained within a 29°C incubator with irregularly
185 pulsating LED lights at ~1.5s intervals to force the *Drosophila* visual system to adapt
186 to new light levels and increase photoreceptor response. Flies were maintained here
187 for 7 days, as this was the age at which *G2019S* mutants had previously shown
188 visual loss (Hindle et al., 2013). Ten flies of each genotype tested (except for *DJ-*
189 *1α^{A72}* where eight were tested) (N=48).

190

191 *Preparation for Electretinogram*

192 On the day of testing, flies were collected using a pooter and aspirated into a
193 shortened pipette. Once the fly's head was protruding from the tip of the pipette, it
194 was restrained by placing a small layer of nail varnish on the back of the fly's neck.
195 Two pipettes at a time were mounted onto a customised *Drosophila*
196 electroretinogram (ERG) recording system, with both flies placed 22cm away from
197 the dual display monitors (West et al., 2015). ERG recordings were made through
198 hollow drawn-glass electrodes containing simple saline (130mM, NaCl, 4.7 mM KCl,
199 1.9mM CaCl₂) connected to a high-impedance amplifier (LF356 op-amp in the circuit
200 [Fig.7] of (Ogden, 1994)) via thin silver wires. The reference electrode was inserted

201 gently onto the *Drosophila* proboscis, and the recording electrode was placed on the
202 surface of the right eye. Ten unique flies of each genotype at each age were tested
203 (total N=250).

204

205 *Stimuli*

206 Stimuli were contrast-reversing achromatic sine wave gratings with a range of
207 Michelson contrasts (Michelson, 1927) and temporal frequencies. Spatial frequency
208 was held at 0.056 cycles per degree as this had previously been found to be the
209 optimal spatial frequency to measure SSVEP recordings from *Drosophila* (West et
210 al., 2015a). Stimuli were generated using the Psychophysics Toolbox on a Windows
211 7 PC and were displayed on dual 144Hz LCD monitors (XL240T, BenQ, Tiwam).
212 Stimuli swept through unique combinations of 8 levels of temporal frequency (1, 2, 4,
213 6, 8, 12, 18 and 36 Hz) and 8 levels of contrast (1, 4, 8, 16, 32, 64, 99%) to generate
214 64 different combinations of temporal contrast stimuli. Parameter combinations were
215 presented in a random order for an 11 second trial, with a 4 second inter-stimulus
216 interval. The first second of each trial was removed prior to analysis to remove onset
217 transients. Each parameter combination was presented 3 times per fly to create a
218 ~1-hour recording session.

219

220 *Analysis*

221 *Steady state visually evoked potentials*

222 The periodic modulation of a contrast reversing grating evokes steady-state,
223 visually evoked potentials (SSVEPs) with a phase-locked, periodic time course which
224 is analysed most conveniently in the frequency domain (see Figure 1A and C for
225 examples of SSVEP response from *w⁻* and *PINK1* mutants). For a single contrast

226 reversing grating, the ERG records responses from both the photoreceptors and the
227 subsequent neuronal signalling pathways (Afsari et al., 2014). Individual
228 photoreceptors will track the luminance modulations of the grating bars at the input
229 frequency (F_1) but because the signal elicited by a grating is a population average of
230 photoreceptors driven by different transition polarities (some dark->light, some light-
231 >dark) the overall photoreceptor contribution is largely self-cancelling. Residual
232 responses at F_1 arise from asymmetries in photoreceptor sampling of the relatively
233 low spatial frequency grating. The majority of the signal is composed of the transient
234 responses arising from the visual neurons which are confined to even multiples of
235 the input frequency. Of these responses, the second harmonic is by far the largest
236 and we restrict our analyses to $2f$ for each input frequency. A coherently averaged
237 (phase-sensitive) Fourier amplitude was calculated for each temporal frequency and
238 contrast combination by averaging complex frequency-domain data obtained for
239 each condition over 3 runs (see Figure 1B and D for examples of Fourier amplitudes
240 from w^- and *PINK1* mutants). Due to the phase-locked nature of VEPs, coherent
241 averaging preserves the signal while phase-randomized noise sums to zero (Norcia
242 et al., 2015). This results in a high signal to noise ratio for SSVEP recordings.

243

244 *FIGURE 1 HERE*

245 *Linear discriminant analysis*

246 We assessed LDA as a tool to accurately assign flies into their correct
247 genotype based on multivariate visual response profiles. We used ERG
248 measurements recorded in response to 64 combinations of contrast and temporal
249 frequency, thus, providing a 64-dimensional dataset to input into the LDA. Each fly
250 was therefore located in a 64-dimensional space. Flies that showed similar

251 responses to these combinations of contrast and temporal frequency clustered
252 together in this space. Thus, if different classes showed different visual responses,
253 unique clusters for each class would form in this 64-dimensional space. The LDA
254 algorithm then attempted to identify a single linear boundary between these clusters
255 and classified each fly into a genotypic class by asking which side of this linear
256 boundary the fly was situated. The accuracy of the LDA algorithm depends on the
257 degree of separation between the genotypic clusters in the multidimensional feature
258 space. This is further expanded upon in Figure 2, where we illustrate the process of
259 raw data collection through to a range of possible classifications.

260

261 *FIGURE 2 HERE*

262

263 **Results**

264 *Early-onset PD temporal contrast profile amplitudes are larger than controls*

265 A series of exemplar raw SSVEP responses from both *w⁻* and *PINK1* mutants
266 at different ages and stimulus contrasts are illustrated in Figure 3. Average Fourier
267 amplitudes at $2f$ for each temporal contrast combination for each genotype are
268 illustrated in Figure 4. Higher peak response amplitudes are represented by lighter
269 colours whilst lower amplitudes are represented by darker colours. Visual response
270 changes as a function of both contrast and temporal frequency, with responses in
271 both wild-type and EOPD models peaking at high contrast (99%) and an
272 intermediate temporal frequency (6-8Hz).

273

274 *FIGURE 3 HERE*

275 *FIGURE 4 HERE*

276

277 *Principal Components Analysis*

278 We computed a Principal Components Analysis (PCA) on the full dataset
279 (N=250) (See Figure 5). This allowed us to retain just those principal components
280 (PCs) that explain significant amounts of the overall variance, simplifying our 64-
281 dimensional data significantly (Jolliffe & Cadima, 2016; West et al., 2015a). Our first
282 PC explained 89.9% of total variance within the dataset and the univariate analysis
283 that follows is based on the amplitude of this component while the multivariate
284 analysis later in the paper is performed on the full dataset.

285

286

FIGURE 5 HERE

287

288 *Main effects*

289 A 5x5 between groups ANOVA was performed on the first principal
290 component score (representing SSVEP amplitude) to assess if there was a
291 difference in SSVEP amplitudes between *Drosophila* genotypes or ages. The
292 analysis found a significant main effect of genotype, $F(4,225) = 21.428$, $p < .001$,
293 indicating a difference in response amplitude between the five genotypes, when
294 collapsed over age. The analysis also found a significant main effect of age $F(4,225)$
295 $= 5,558$, $p < .001$, indicating a difference in response amplitude between the 5 ages,
296 when collapsed over genotype. Finally, there was a significant interaction effect
297 $F(16,225) = 2.984$, $p < .001$, indicating that response amplitude differed between
298 genotype depending on age. A simple effects analysis was performed to tease out
299 differences in our conditions and explore our interaction effect.

300

301 *Simple effects analysis comparing between genotypes within each age group*

302 A simple effects analysis was undertaken to explore differences in the SSVEP
303 amplitudes of *Drosophila* genotypes within each age group, with Sidak corrections
304 applied to all possible comparisons. The SSVEP amplitudes of each genotype as a
305 function of age are illustrated in Figure 6, whilst all corresponding p values are
306 presented in Statistical Supplements Tables 1-10. Analysis revealed that at 1 day
307 of age, all EOPD mutations (i.e. excluding $dLRRK^{ex1}$) had significantly higher SSVEP
308 amplitudes when compared to w^- control flies, ($p < .01$). When comparing between 1
309 day old PD mutants, $PINK1^5$ produced significantly higher SSVEP amplitudes when
310 compared to both $DJ-1\alpha^{\Delta 72}$ ($p < .05$) and $dLRRK^{ex1}$ mutants ($p < .01$). There were no
311 other significant differences in the SSVEP amplitudes of PD mutants. The larger
312 amplitudes of EOPD mutants did not hold over later ages as wild type response
313 increased at 7 days of age (see Figure 6). However, differences between the SSVEP
314 amplitudes of PD mutants was found at these later ages. At 7 days of age $PINK1^5$
315 mutants produced significantly higher amplitudes when compared to $dLRRK^{ex1}$ ($p <$
316 $.005$), whilst at 14 days of age $DJ1-\beta^{\Delta 93}$ had significantly higher amplitudes when
317 compared to $DJ-1\alpha^{\Delta 72}$ ($p < .001$) and $dLRRK^{ex1}$ ($p < .001$) mutants. This trend
318 continued at 21 days of age, with $DJ1-\beta^{\Delta 93}$ continuing to show higher SSVEP
319 amplitudes when compared to $DJ-1\alpha^{\Delta 72}$ ($p < .01$) and $dLRRK^{ex1}$ ($p < .05$). At 28
320 days of age, $DJ1-\beta^{\Delta 93}$ ($p < .01$) and $PINK1^5$ ($p = .01$) produced significantly higher
321 SSVEP amplitudes when compared to $DJ-1\alpha^{\Delta 72}$.

322

323

FIGURE 6 HERE

324

325 *Simple effects analysis comparing between age group within each genotype*

326 A simple main effects analysis was undertaken to explore differences in the
327 SSVEP amplitudes within each *Drosophila* genotype over its lifespan, with Sidak
328 corrections applied to all possible comparisons. The p values for all simple effects
329 are presented in Supplements. Analysis revealed that w^- response amplitudes
330 increased between 1 and 7 days of age ($p = .001$), however there was no significant
331 difference when comparing between further consecutive ages within this genotype,
332 thus, visual response held stable between 7 to 28 days of age. There was a
333 significant increase in $DJ1-\beta^{A93}$ response amplitudes between 7 and 14 days of
334 age ($p < .001$), which then held steady from 14 to 28 days of age. There was no
335 significant difference in response amplitudes within $DJ-1\alpha^{A72}$, $PINK1^5$ or $dLRRK^{ex1}$
336 at any consecutive ages between 1 and 28 days.

337

338 *Increased demand for energy in the visual system leads to loss of visual response in*
339 *old PD flies*

340 While we demonstrated that abnormal gain control occurs in 1 day old EOPD
341 mutants, at later ages, responses were comparable to those of wild-type flies (w^-).
342 This represents a difference between EOPD mutant flies and flies mimicking the late-
343 onset *LRRK2-G2019S* mutation, where responses fall to zero at later ages (Hindle et
344 al., 2013). We hypothesized that maintaining our *Drosophila* stocks at 25° and a
345 12:12 LD cycle did not produce enough neuronal demand on the visual system to
346 see any effect. To test this hypothesis, we increase the demand for energy by
347 exposing *Drosophila* to irregular ~1.5s flashes of light of at random periodic intervals
348 over seven days. Here, we hypothesise that the abnormal gain we have observed in
349 young EOPD flies will interact with a visually induced increase in neural demand to
350 cause an excitotoxic cascade.

351 Observation of temporal contrast response profiles (see Figure 7) indicated a
352 profound reduction in SSVEP amplitudes across temporal frequency and contrast
353 combinations for PD mutants (but not wild-type flies) after seven days exposure to
354 photic stress.

355

356 *FIGURE 7 HERE*

357

358 A one way between groups ANOVA was performed on the first principal
359 component score (representing SSVEP amplitude) extracted via the PCA analysis to
360 assess if there was a significant difference in visual response between five
361 *Drosophila* genotypes after they had been exposed to seven days of photic stress.
362 The analysis found a significant main effect of genotype, $F(1,43) = 5.965$, $p = .001$,
363 $\eta^2 = .357$, indicating a difference in response amplitude between the five genotypes.
364 Pairwise comparisons revealed that all PD mutants produced significantly lower
365 SSVEP amplitudes when compared to w^- control flies ($p < .05$), indicating an
366 interaction between visual stimulation and *Drosophila* genotype on visual response
367 amplitudes (see Figure 8). There was no significant difference between the PD
368 mutants' SSVEP responses.

369

370 *FIGURE 8 HERE*

371

372 *Linear discriminant analysis classifies flies into their correct genotypic class*

373 Thus, all EOPD mutants show both an early increased visual response and a
374 loss of vision after 7 days of visual stimulation, compared to w^- control flies.

375

376 In the presentation of our data so far, we utilized PCA to reduce the
377 dimensionality in our data to a single variable, thereby removing any nuanced
378 differences between full *Drosophila* temporal contrast profiles. We now explore how
379 linear discriminant analysis can use the additional small, but significant sources of
380 variation in our SSVEP data to classify *Drosophila* into their correct genotypic class
381 and age group.

382

383 Linear Discriminant Analysis (LDA) is a statistical method that aims to answer
384 both binary and multi-class classification problems by seeking linear combinations of
385 variables that best explain the variance within the data, working under the
386 assumption that unique classes generate unique Gaussian distributions (Izenman,
387 2008). We assess the accuracy of our LDA in two ways. First, we use a standard
388 linear classifier (Fisher, 1936) as implemented in MATLAB's (2017a, Mathworks,
389 MA) 'classify' function to conduct a leave one out (LOO) analysis, where the
390 classifier receives training data from all flies to be assessed except one, then we
391 measure the classifiers accuracy in classifying the excluded fly. This fly is
392 resubstituted and the classification is repeated for every fly in the dataset to return a
393 generalized LOO accuracy. Second, use MATLAB's classification function 'fitcdiscr'
394 to fit an LDA model to our raw 64-dimensional data. We then use Monte Carlo
395 resampling methods to produce 3 estimates of accuracy – an overall model
396 accuracy, an N-way classification accuracy (the accuracy of correctly classifying a fly
397 into one of the 5 genotypes at each age group or 5 age groups for each genotype)
398 and a pair-wise classification accuracy (the accuracy of correctly classifying a fly into
399 one of two correct genotypes at each age group). For detailed description of the

400 methods we used to apply LDA to multivariate *Drosophila* data, please see West et
401 al. (2015).

402 Here, we hypothesise that *Drosophila* will be classified into their correct
403 genotypic class at above-chance levels based on temporal contrast profiles, in line
404 with previous findings using spatiotemporal profiles (West et al., 2015a).

405

406 *Overall Model Discrimination Accuracy*

407 We first ran our full dataset of 25 classes through the LDA to assess how well
408 it could classify *Drosophila* when considering both their genotype and age. In this
409 case, baseline (chance) performance was 4% (1/25). Next, to assess how well we
410 could discriminate between *Drosophila* genotypes within each age group, our data
411 were partitioned into 5 genotypes and LDA was applied with a 20% chance baseline
412 (1/5). Finally, to assess how well we could classify between *Drosophila* at different
413 ages within each genotype, our data were divided into 5 age groups within each
414 genotype and analysed using LDA, again with a 20% chance baseline (1/5).

415

416 The full overall classification accuracies for both LOO analysis and Monte
417 Carlo resampling analysis for all 3 sets of data are presented in Table 11. The
418 overall accuracy of our model in classifying *Drosophila* into their correct genotypic
419 class differed depending on the age of the genotypes included in the model. The
420 highest classifications occurred at 1 and 28 days of age. Although there was a slight
421 decrease in accuracies when classifying *Drosophila* into their correct age within a
422 genotype, the algorithm still performed above 20% chance baseline for all
423 genotypes.

424

Class	LOO Classification	Monte Carlo Resampling
All 25 classes	24.8%	29.6%
1 day post eclosion	58%	68%
7 days post eclosion	52%	64%
14 days post eclosion	46%	54%
21 days post eclosion	48%	50%
28 days post eclosion	64%	70%
w^-	54%	54%
$DJ-1\alpha^{\Delta 72}$	38%	38%
$DJ1-\beta^{\Delta 93}$	52%	52%
$PINK1^5$	34%	50%
$dLRRK^{ex1}$	26%	34%

425

426 Table 11: Classification accuracy differs when flies are grouped by age and
427 classified into genotype, and when they are grouped by genotype and classified into
428 age. Generally, both LOO and Monte Carlo resampling methods provide similar
429 classification accuracies. N=50 for per class (chance baseline 20%), except 'All 25
430 classes' N=250 (chance baseline 4%).

431

432 *N-Way Classification Accuracy*

433 The confusion matrix was used to establish the accuracy of our LDA model to
434 classify *Drosophila* into their correct genotypic class. Again, we investigated the
435 precision of our model when all 25 classes were included in the model, with a 4%
436 chance baseline (1/25). All classifications were reported above chance, bar $PINK1^5$
437 at 21 days of age. The highest accuracy was for w^- at 1 day of age, where the

438 model performed with 34.49% accuracy, whilst most other conditions were classified
439 with ~25% accuracy. A profile of classification accuracies when all 25 classes are
440 considered is presented in Figure 9.

441

442

FIGURE 9 HERE

443

444 Next, we assessed the ability of the classifier to accurately genotype
445 *Drosophila* within each age group, thus, five genotypes at each age were included in
446 the model, with a 20% chance baseline (1/5). Our classification accuracy is deduced
447 by normalizing our confusion matrix by dividing by the number of flies in each
448 condition (n=10). As illustrated in Figure 10, at 1 day of age our model could classify
449 w^- control flies into their correct genotypic class with 78.8% accuracy, whilst we
450 could classify $DJ-1\alpha^{\Delta 72}$ at 45.5% accuracy, $DJ1-\beta^{\Delta 93}$ at 52.9% accuracy, $PINK1^5$ at
451 73.6% accuracy and $dLRRK^{ex1}$ at 60.0% accuracy.

452

453

FIGURE 10 HERE

454

455 These accuracies shifted at seven days of age, with our model classifying w^-
456 with 29.8% accuracy, $DJ-1\alpha^{\Delta 72}$ with 50.0% accuracy, $DJ1-\beta^{\Delta 93}$ with 64.7%
457 accuracy, $PINK1^5$ with 62.2% accuracy and $dLRRK^{ex1}$ at 46.9% accuracy. At 14
458 days of age our model could accuracy classify w^- at 50.0% accuracy, $DJ-1\alpha^{\Delta 72}$ at
459 68.1% accuracy, $DJ1-\beta^{\Delta 93}$ at 50.3% accuracy, $PINK1^5$ at 36.4% accuracy and
460 $dLRRK^{ex1}$ at 29.1% accuracy. At 21 days of age with our model classified w^- at
461 58.35% accuracy, $DJ-1\alpha^{\Delta 72}$ at 50.5% accuracy, $DJ1-\beta^{\Delta 93}$ at 50.2% accuracy,
462 $PINK1^5$ at 25.7% accuracy and $dLRRK^{ex1}$ 53.8% accuracy. At 28 days of age our

463 model classified w^- with 53.7% accuracy, $DJ-1\alpha^{\Delta 72}$ with 71.5% accuracy, $DJ1-\beta^{\Delta 93}$
 464 with 62.6% accuracy, $PINK1^5$ with 55.1% accuracy and $dLRRK^{ex1}$ at 46.35%
 465 accuracy.

466

467 *N-Way Classification Accuracy: Age*

468 Here, our LDA model was used to classify *Drosophila* mutants into their
 469 correct age within a single genotype, with a 20% chance baseline (1/5).
 470 Comparatively, the model was generally weaker in accurately classifying into age
 471 when compared to classifying into genotype, although all classifications exceeded
 472 chance baseline. Age N-Way classification accuracies for each genotype are
 473 presented in Table 12.

474

N-Way Classification Accuracy

Genotype	1 day	7 days	14 days	21 days	28 days
w^-	81.3%	29.5%	32%	53.5%	53.5%
$DJ-1\alpha^{\Delta 72}$	26.6%	34.1%	50.0%	29.7%	48.4%
$DJ1-\beta^{\Delta 93}$	55.3%	59.5%	51.0%	45.0%	57.3%
$PINK1^5$	39.7%	49.1%	35.0%	27.2%	49.3%
$dLRRK^{ex1}$	37.6%	23.7%	22.7%	30.2%	43.7%

475 Chance baseline: 20% (1/5)

476 Table 12: N-Way classification of flies into their correct age differs between
 477 genotypes. All classes can be classified above 20% chance baseline, with the
 478 highest accuracy sitting at 81.3% for 1 day old w^- classifications. n=10

479

480

481 *Pairwise Classification Accuracy*

482 To assess the accuracy of our model in classifying *Drosophila* between pairs
 483 of genotypes within each age group we bootstrapped our data through 1000
 484 iterations of a two-way classification analysis. Here, we assess the accuracy of the
 485 algorithm estimation in classifying a fly from a pair of genotypes into its correct class.
 486 Classification is significantly above chance when fewer than 5% of the bootstrapped
 487 2-way classification probabilities are .5 or greater.

488

489 As presented in Table 13, the algorithm classified one-day old *Drosophila*
 490 genotypes with accuracy between 73.7% - 94.1% ($p < .05$). Notably, all PD mutants
 491 could be accurately distinguished from w^- control flies.

492

	w^-	<i>DJ1-β</i> ^{Δ93}	<i>DJ-1α</i> ^{Δ72}	<i>dLRRK</i> ^{ex1}
<i>PINK1</i> ⁵	94.1%*	84.7%*	78.8%*	88.9%*
w^-	-	86.3%*	75.8%*	77.6%*
<i>DJ1-β</i> ^{Δ93}	-	-	57.9%	73.7%*
<i>DJ-1α</i> ^{Δ72}	-	-	-	65.3%

493 * = $p < .05$

494 Table 13: LDA can accurately compute pairwise classifications between PD and
 495 control genotypes at 1 day of age (n=10).

496

497 As presented in Table 14, at 7 days of age the model had a reduction in the
 498 amount of significant comparisons, performing between 74.5% - 85.6% accuracy. At
 499 this age, the LDA could not accurately discriminate between any of the PD mutants
 500 and control flies.

	w^-	$DJ1-\beta^{\Delta 93}$	$DJ-1\alpha^{\Delta 72}$	$dLRRK^{ex1}$
$PINK1^5$	69.9%	74.7%*	76.1%*	85.6%*
w^-	-	60.8%	60.5%	63.3%
$DJ1-\beta^{\Delta 93}$	-	-	67.7%	76.3%*
$DJ-1\alpha^{\Delta 72}$	-	-	-	66.9%

* = $p < .05$

501

502 Table 14: LDA had a reduction in total significant comparisons at 7 days of age, and
503 cannot accurately discriminate between any of the PD mutants when compared
504 against control flies (n=10).

505

506 At 14 days of age there appeared to be an overall improvement in pairwise
507 classifications with significant pairwise classifications between 78.0% - 81.3%
508 accuracy, as illustrated in Table 15.

509

	w^-	$DJ1-\beta^{\Delta 93}$	$DJ-1\alpha^{\Delta 72}$	$dLRRK^{ex1}$
$PINK1^5$	61.7%	57.8%	78.6%*	79.2%*
w^-	-	78.4%*	78.0%*	79.9%*
$DJ1-\beta^{\Delta 93}$	-	-	89.6%*	91.3%*
$DJ-1\alpha^{\Delta 72}$	-	-	-	52.1%

* = $p < .05$

510

511 Table 15. LDA can accurately compute pairwise classifications between PD and
512 control genotypes at 14 days of age (n=10). There are differences in accuracy when
513 compared to 7 and 1 day old classifications.

514

515 This held at 21 days of age, where our pairwise classification accuracy
 516 reached between 75.2% - 85.1% for significant comparisons, as illustrated in Table
 517 16, however there was a reduction in significant comparisons at this age.

	w^-	$DJ1-\beta^{\Delta 93}$	$DJ-1\alpha^{\Delta 72}$	$dLRRK^{ex1}$
$PINK1^5$	63.3%	65.2%	75.2%*	52.9%
w^-	-	78.4%*	77.4%*	69.4%
$DJ1-\beta^{\Delta 93}$	-	-	85.1%*	77.7%*
$DJ-1\alpha^{\Delta 72}$	-	-	-	60.6%

518 * = $p < .05$

519 Table 16. LDA can accurately compute pairwise classifications between PD and
 520 control genotypes at 21 day of age (n=10), however there are less significant
 521 comparisons compared to earlier ages.

522

523 In line with our peak in overall model accuracy, our model was most accurate
 524 in classifying between flies at 28 days of age, with all possible comparisons
 525 statistically significant and sitting between 72.7% and 86.2% accuracy (Table 17).
 526 Similar to one day old comparisons, all PD mutants could be accurately
 527 distinguished from w^- control flies at 28 days of age. We note that these statistics
 528 differ from the comparisons on the PCA simple effects analysis data, as will be
 529 addressed in our discussion.

530

531

532

533

	w^-	$DJ1-\beta^{\Delta 93}$	$DJ-1\alpha^{\Delta 72}$	$dLRRK^{ex1}$
$PINK1^5$	78.9%*	78.7%*	79.7%*	73.7%*
w^-	-	86.2%*	81.0%*	75.6%*
$DJ1-\beta^{\Delta 93}$	-	-	88.4%*	83.6%*
$DJ-1\alpha^{\Delta 72}$	-	-	-	72.7%*

* = $p < .05$

534

535 Table 17. LDA accurately computes pairwise classifications between all genotypes at
536 28 days of age (n=10). All comparisons are significant and above 72.7% accuracy.

537

538

Discussion

539 *Abnormal gain control in early-onset PD Drosophila models*

540 We have demonstrated that abnormal gain control occurs in young EOPD
541 mutants; $DJ-1\alpha^{\Delta 72}$, $DJ1-\beta^{\Delta 93}$, and $PINK1^5$. *Drosophila* with these mutations have
542 significantly higher SSVEP response amplitudes when compared to w^- controls at
543 day 1. Notably, there appears to be no difference between response amplitudes of 1
544 day old w^- controls and knockout of the fly *LRRK2* homologue $dLRRK^{ex1}$. These
545 results are consistent with previous studies, and point to a common phenotype of
546 abnormal gain control occurring in the current studied EOPD mutants and the
547 *LRRK2-G2019S* late-onset mutant (Afsari et al., 2014; West et al., 2015a).

548

549 What common biological mechanism might explain these findings?
550 Dopaminergic terminals are found in the *Drosophila* ommatidium, lamina, and
551 medulla, where dopamine is thought to regulate contrast sensitivity, light adaptation,
552 and circadian rhythms (Afsari et al., 2014; Chyb et al., 1999; Hirsh et al., 2010;
553 Jackson et al., 2012; Nassel & Elekes, 1992). Thus, dopamine acts as a

554 neuromodulator within the *Drosophila* visual system, effectively regulating neural
555 response to visual excitation. PD-model flies may have less dopamine content,
556 and/or fewer dopaminergic neurons, or disrupted dopamine signalling, though the
557 reduction may depend on the environmental conditions (Navarro et al., 2014; Ng et
558 al., 2012; Park et al., 2006; Wang et al., 2006). Any reduction in dopamine release
559 will cause photoreceptors to respond faster and with greater amplitude (Chyb et al.,
560 1999). This hyperactivity causes increased SSVEP amplitudes, manifesting as
561 abnormal gain control. Humans, like flies, have retinal dopamine within the amacrine
562 cells and inner border of the nuclear layer, where it is thought to be responsible for
563 light adaptation, contour perception, and contrast sensitivity (Crooks & Kolb, 1992;
564 Dowling, 1979; Witkovsky, 2004). Human patients also show a reduction in retinal
565 dopamine and report a range of low-level visual deficits, including poor contrast
566 sensitivity and reduced light sensitivity (Archibald, Clarke, Mosimann, & Burn, 2011;
567 Beitz, 2014; Chaudhuri & Schapira, 2009; Weil et al., 2016). These homologies in
568 retinal structure, function, and disease pathology point to the possibility that
569 prodromal gain control abnormalities occur in human PD patients.

570

571 The response profile of wild-type w^- *Drosophila* changes as a function of age.
572 This genotype initially presented with comparatively low response amplitudes when
573 compared to EOPD mutants. w^- response then increased between 1 and 7 days of
574 age. This reflects the anatomical plasticity of the young *Drosophila* visual system.
575 Young w^- flies are born with reduced visual sensitivity which then adapts to
576 functional requirements, with visual maturity occurring between 4 - 7 days of age
577 (Kral & Meinertzhagen, 1989). It is important to note that all *Drosophila* included in
578 our study are white eyed, thus share the w^- mutation. The increased sensitivity to

579 visual stimuli we observe in EOPD mutants, and mutants' unique developmental
580 profiles, is due solely to the PD mutation.

581

582 *Excitotoxicity as a pathological phenotype in Parkinson's disease*

583 Initially we saw no evidence of excitotoxic damage in the visual system of
584 older PD flies. However, *Drosophila* in the lab experience a relatively stable visual
585 environment: light levels are many orders of magnitude lower than those in the
586 outside world and they are modulated according to a strict 12hr:12hr LD cycle. We
587 theorised that purposeful visual stimulation of the PD *Drosophila* visual system may
588 be necessary to induce excitotoxicity in the lab. To increase neural demand for
589 energy we exposed flies to a rich visual environment which contained irregular bursts
590 of high intensity luminance modulations. This environment requires the
591 photoreceptors both to change their firing rates and their mean sensitivity over
592 relatively short time periods. Our hypothesis was that the abnormal gain control we
593 observed in young EOPD flies would interact with an increase in neural activity to
594 cause an excitotoxic cascade. Our data are consistent with this hypothesis – PD, but
595 not w^- flies, showed reduced visual functionality after prolonged exposure to these
596 visually demanding environments.

597

598 Our results provide evidence for an excitotoxic cascade in PD *Drosophila*
599 mutants, with $DJ-1^{\Delta 72}$, $DJ1-\beta^{\Delta 93}$, and $PINK1^5$ all showing a significant decrease in
600 SSVEP amplitudes after seven days of visual stimulation, with a minimum of 50%
601 reduction in response. Surprisingly, the response amplitudes of $dLRRK^{ex1}$ mutants
602 were also reduced, even though we did not observe abnormal gain control in this
603 strain at one day of age.

604

605 We draw upon the previously established theory of excitotoxicity in PD explain
606 the biological processes underlying our observed visual loss. Here, abnormal gain
607 control interacts with a visually induced increase in neural demand. This causes an
608 increase in ionic flux across the cell membrane which in turn results in extra demand
609 for ATP from the ion exchange pumps. When mitochondria cannot meet this
610 increased demand for ATP, they release reactive oxygen species (e.g. superoxide,
611 hydrogen peroxide), so generating oxidative stress, which leads to autophagy,
612 apoptosis and other forms of cell damage. This is then followed visual decline and
613 eventual cell death (Hindle et al., 2013).

614

615 Mitochondrial dysfunction and oxidative stress appear to play a central role in
616 PD pathogenesis (Bogaerts, Theuns, & Van Broeckhoven, 2008; Büeler, 2009;
617 Henchcliffe & Beal, 2008; Schapira, 2008). The current paper has investigated
618 *Drosophila* PD mutations in genes whose human homologues are associated with
619 EOPD. In both humans and flies, *DJ-1* encodes a small protein that is thought to
620 protect against oxidative stress and assist in mitochondrial regulation by acting as a
621 sensor for Reactive Oxidative Species (ROS) (Oswald et al., 2016). Subsequently,
622 loss-of-function mutations in *DJ-1* appear to increase cell death in response to
623 oxidative stress. Further, animal studies have observed perturbations in dopamine
624 release in DJ-1 deficient animal models, although there is no physiological loss of
625 dopamine neurons (Goldberg et al., 2005; Martella et al., 2011; Menzies, Yenissetti, &
626 Min, 2005; Meulener et al., 2005; Pisani et al., 2006; Yang, Chen, Ding, Zhuang, &
627 Kang, 2007). *PINK1* is a protein kinase with a mitochondrial targeting sequence and
628 acts to maintain mitochondrial homeostasis in dopaminergic neurons (Park et al.,

629 2006). Likewise, studies in *PINK1* animal models have found evidence for abnormal
630 mitochondrial morphology and impaired dopamine release (Clark et al., 2006; Kitada
631 et al., 2007; Park et al., 2006). Thus, the protein products of both *DJ-1* and *PINK1*
632 both play roles in the regulation of cellular energy production. However, loss-of-
633 function mutations on these genes negatively impact mitochondria in different ways.
634 Our data provide additional support for the hypothesis that mitochondrial impairment
635 plays a role in the pathogenesis of genetic PD.

636

637 *Classification of Drosophila PD genotype*

638 Previously, we demonstrated that discriminant analysis is a useful tool that
639 can accurately classify PD *Drosophila* into their correct genotypic class at 1 day of
640 age (West et al., 2015a). Here, we build upon this observation, establishing that
641 variability within temporal contrast response profiles obtained from *Drosophila* can
642 be used in a LDA to accurately classify *Drosophila* into their correct genotypic class
643 at various ages with above chance accuracy. When all 25 classes were included in
644 our model, our LOO classification accuracy sat at 24.8%, whilst our bootstrapped
645 classification accuracy was 29.6% (chance baseline of 4%). Our LDA model also
646 performed well when classifying five genotypes within a single age group. Highest
647 classifications occurred at one day (Monte Carlo sampling accuracy of 68% and LLO
648 accuracy of 58%) and 28 days of age (Monte Carlo sampling accuracy of 70% and
649 LOO accuracy of 64%) with a baseline of 20%. This indicates that there are
650 substantial differences between *Drosophila* genotypes at both one and 28 days of
651 age.

652

653 When all 25 classes were included in our model, all classifications (except
654 *PINK1*⁵) perform above a 4% chance baseline, with most classifications occurring
655 with ~25% accuracy. There is substantial variation between PD *Drosophila* visual
656 response throughout their lifespan, indicating that EOPD mutations have unique
657 effects on *Drosophila* visual pathways at not only one day of age, but throughout the
658 *Drosophila* lifespan. After our data were partitioned into five genotypes for each age
659 group, we could classify *Drosophila* into their correct genotypic class with 29.8% -
660 78.8% accuracy over all possible age groups, with no classifications falling under the
661 statistical chance baseline of 20%. Our results illustrate that mutants can be
662 accurately classified into their correct genotypic class beyond one day of age,
663 indicating there are subtle differences in how EOPD mutations affect *Drosophila*
664 neural gain control, as will be discussed.

665

666 Although the N-Way classification accuracy decreased when the algorithm
667 was required to classify *Drosophila* into their correct age within a single genotype,
668 our model still performed above chance baseline. This is surprising considering the
669 results of our first experiment, where, for the most part, within genotype responses
670 did not significantly differ over time. Our analysis was run on a reduced number of
671 genotypes and flies (n=10 and five genotypes, rather than n=20 and 10 genotypes
672 as per West et al. (2015)), yet our model produced a consistently high classification
673 accuracy, even with all 25 classes were included in the model. In West et al., (2015),
674 we varied temporal and spatial frequency but kept contrast fixed. We observed
675 relatively little dependence on spatial frequency up to a hard cut-off that was
676 associated with spatial sampling limits. Our use of contrast rather than spatial
677 frequency in the experiments described here allows us to measure the full contrast

678 sensitivity profile of each genotype and age, increasing the sensitivity of this
679 multivariate visual biomarker for EOPD genes in *Drosophila*. Further, our assay,
680 when combined with LDA, is sensitive enough to detect small differences in the
681 effect of EOPD mutations on *Drosophila* neural gain control. Our initial analysis
682 found a substantial difference between w^- and EOPD mutants at 1 day of age,
683 however our LDA results indicate that these mutations have their own subtle effects
684 on neural gain control across *Drosophila* lifespan. Our findings carry an important
685 implication. As noted, *DJ-1* acts as a ROS sensor, whilst *PINK1* acts to maintain
686 mitochondrial homeostasis in dopaminergic neurons (Lavara-Culebras, Muñoz-
687 Soriano, Gómez-Pastor, Matallana, & Paricio, 2010; Oswald et al., 2016; Park et al.,
688 2006). The ability of our LDA to accurately distinguish between mutations on these
689 genes indicates each mutation uniquely impacts the underlying cellular processes
690 thereby causing a subtle, dissimilar neural responses across *Drosophila* lifespan,
691 that then results in a common pathogenic outcome of visual loss and cell death.

692

693 A key benefit of using *Drosophila* as disease model is their convenience for
694 early-stage drug testing due to their fecundity and fast generation time. It is
695 advantageous to have phenotypic expression of PD mutations at early stages of
696 *Drosophila* lifespan as this supports their utility as an initial model for the rapid
697 testing of neuroactive drugs that have the potential to treat human disease. Like
698 *Drosophila*, perturbations in contrast sensitivity occur in human PD patients due to
699 reduced dopamine levels within the retina (Harnois & Di Paolo, 1990). Our current
700 findings may correspond to the changes seen in human PD patients, although there
701 is obvious difficulty in assessing whether a prodromal abnormal gain control occurs
702 in the early stages of pre-genotyped PD patients. We believe that it may be possible

703 for LDA to classify human PD patients genotype based on multivariate SSVEP
704 response profiles as measured by electroencephalogram (EEG). This would have
705 the potential to assist in early PD diagnosis, genotypic classification, and disease
706 expression. Our next step is to investigate *Drosophila* response to additional low
707 level visual parameters such as chromatic contrast and orientation, and deduce
708 whether a similar biomarker can be established in human PD patients.

709

710 Together, our experiments have uncovered abnormal gain control and an
711 excitotoxic cascade as a common pathological phenotype in three EOPD mutations,
712 *DJ-1* $\alpha^{\Delta 72}$, *DJ1* $\beta^{\Delta 93}$, and *PINK1*⁵. In addition to furthering the link between abnormal
713 gain control and excitotoxicity in genetic forms of PD, our findings have built upon
714 the utility of LDA in genotyping *Drosophila* based on multivariate response profiles.
715 Further, we have illustrated that there are variations in how these EOPD mutations
716 affect neural gain control across *Drosophila* lifespan, indicating that these mutations
717 have unique effects upon underlying cellular processes that lead to a common
718 outcome – visual loss and cell death. Overall, it appears that these PD related
719 mutations are heterochronic: in young flies, mutations lead to stronger neural
720 signalling (increased sensory response may be beneficial in escaping behaviour) but
721 are detrimental in older flies (a loss of vision would hinder escape behaviour)
722 (Himmelberg, West, Wade, & Elliott, 2017). Should these findings in fly models prove
723 applicable to the human situation, it would suggest that prodromal PD may be linked
724 to changes in central nervous system processing that could, potentially, confer
725 advantages in early life at the cost of degenerative disease in old age.

726

727 **Acknowledgments:** We would like to thank Dr Sean Sweeny and Dr Alex Whitworth
728 who generously donated fly stocks used in the study.

729

730 **Grants:** M.M.H was supported by the European Union's Horizon 2020 research and
731 innovation programme under the Marie Skłodowska-Curie grant agreement No
732 641805. R.J.H.W developed the original equipment and methods under support from
733 the Wellcome Trust and the York Centre for Chronic Diseases and Disorders
734 (C2D2).

735

736 **Disclosures:** No conflicts of interest, financial or otherwise, are declared by the
737 authors.

738

739 **Author Contributions:** Data were collected by M.M.H. All authors contributed to the
740 design, implementation and analysis as well as writing the paper.

741

742

743

744

745

746

747

748

749

750

751

752
753
754
755
756
757
758
759
760
761
762
763
764
765
766
767
768
769
770
771
772
773
774
775
776

References

Afsari, F., Christensen, K. V., Smith, G. P., Hentzer, M., Nippe, O. M., Elliott, C. J. H., & Wade, A. R. (2014). Abnormal visual gain control in a Parkinson's disease model. *Human Molecular Genetics*, *23*(17), 12. <https://doi.org/10.1038/nrn2619>

Archibald, N. K., Clarke, M. P., Mosimann, U. P., & Burn, D. J. (2011). Visual symptoms in Parkinson's disease and Parkinson's disease dementia. *Movement Disorders*, *26*(13), 2387–2395. <https://doi.org/10.1002/mds.23891>

Beal, M. F., Brouillet, E., Jenkins, B. G., Ferrante, R. J., Kowall, N. W., Miller, J. M., ... Hyman, B. T. (1993). Neurochemical and histologic characterization of striatal excitotoxic lesions produced by the mitochondrial toxin 3-nitropropionic acid. *The Journal of Neuroscience : The Official Journal of the Society for Neuroscience*, *13*(October), 4181–4192.

Beitz, J. M. (2014). Parkinson's disease: a review. *Frontiers in Bioscience (Scholar Edition)*, *6*, 65–74. <https://doi.org/10.2741/S415>

Bogaerts, V., Theuns, J., & Van Broeckhoven, C. (2008). Genetic findings in Parkinson's disease and translation into treatment: A leading role for mitochondria? *Genes, Brain and Behavior*. <https://doi.org/10.1111/j.1601-183X.2007.00342.x>

Büeler, H. (2009). Impaired mitochondrial dynamics and function in the pathogenesis of Parkinson's disease. *Experimental Neurology*. <https://doi.org/10.1016/j.expneurol.2009.03.006>

Busse, L., Wade, A. R., & Carandini, M. (2009). Representation of Concurrent Stimuli by Population Activity in Visual Cortex. *Neuron*, *64*(6), 931–942. <https://doi.org/10.1016/j.neuron.2009.11.004>

Carandini, M., & Heeger, D. (1994). Summation and division by neurons in primate

777 visual cortex. *Science (New York, N.Y.)*, 264(5163), 1333–1336.
778 <https://doi.org/10.1126/science.8191289>

779 Carandini, M., & Heeger, D. J. (2011). Normalization as a canonical neural
780 computation. *Nature Reviews Neuroscience*. <https://doi.org/10.1038/nrn3136>

781 Carandini, M., Heeger, D. J., & Movshon, J. A. (1997). Linearity and normalization in
782 simple cells of the macaque primary visual cortex. *The Journal of*
783 *Neuroscience : The Official Journal of the Society for Neuroscience*, 17(21),
784 8621–8644.

785 Chaudhuri, K. R., & Schapira, A. H. (2009). Non-motor symptoms of Parkinson's
786 disease: dopaminergic pathophysiology and treatment. *The Lancet Neurology*.
787 [https://doi.org/10.1016/S1474-4422\(09\)70068-7](https://doi.org/10.1016/S1474-4422(09)70068-7)

788 Chyb, S., Hevers, W., Forte, M., Wolfgang, W. J., Selinger, Z., & Hardie, R. C.
789 (1999). Modulation of the light response by cAMP in Drosophila photoreceptors.
790 *The Journal of Neuroscience : The Official Journal of the Society for*
791 *Neuroscience*, 19(20), 8799–8807.

792 Clark, I. E., Dodson, M. W., Jiang, C., Cao, J. H., Huh, J. R., Seol, J. H., ... Guo, M.
793 (2006). Drosophila pink1 is required for mitochondrial function and interacts
794 genetically with parkin. *Nature*, 441(7097), 1162–6.
795 <https://doi.org/10.1038/nature04779>

796 Clarke, C. E. (2007). Parkinson's disease. *BMJ (Clinical Research Ed.)*, 335(7617),
797 441–5. <https://doi.org/10.1136/bmj.39289.437454.AD>

798 Crooks, J., & Kolb, H. (1992). Localization of GABA, glycine, glutamate and tyrosine
799 hydroxylase in the human retina. *Journal of Comparative Neurology*, 315(3),
800 287–302. <https://doi.org/10.1002/cne.903150305>

801 de Rijk, M. C., Tzourio, C., Breteler, M. M., Dartigues, J. F., Amaducci, L., Lopez-

802 Pousa, S., ... Rocca, W. A. (1997). Prevalence of parkinsonism and Parkinson's
803 disease in Europe: the EUROPARKINSON Collaborative Study. European
804 Community Concerted Action on the Epidemiology of Parkinson's disease.
805 *Journal of Neurology, Neurosurgery, and Psychiatry*, 62(1), 10–5.
806 <https://doi.org/10.1136/jnnp.62.1.10>

807 Dowling, J. E. (1979). A new retinal neurone - the interplexiform cell. *Trends in*
808 *Neurosciences*, 2(C), 189–191. [https://doi.org/10.1016/0166-2236\(79\)90076-6](https://doi.org/10.1016/0166-2236(79)90076-6)

809 Fisher, R. A. (1936). The use of multiple measures in taxonomic problems. *Annals of*
810 *Eugenics*, 7(2), 179–188. <https://doi.org/10.1111/j.1469-1809.1936.tb02137.x>

811 Goldberg, M. S., Pisani, A., Haburcak, M., Vortherms, T. A., Kitada, T., Costa, C., ...
812 Shen, J. (2005). Nigrostriatal dopaminergic deficits and hypokinesia caused by
813 inactivation of the familial parkinsonism-linked gene DJ-1. *Neuron*, 45(4), 489–
814 496. <https://doi.org/10.1016/j.neuron.2005.01.041>

815 Harnois, C., & Di Paolo, T. (1990). Decreased dopamine in the retinas of patients
816 with Parkinson's disease. *Investigative Ophthalmology and Visual Science*,
817 31(11), 2473–2475.

818 Henchcliffe, C., & Beal, M. F. (2008). Mitochondrial biology and oxidative stress in
819 Parkinson disease pathogenesis. *Nature Clinical Practice. Neurology*, 4(11),
820 600–609. <https://doi.org/10.1038/ncpneuro0924>

821 Himmelberg, M. M., West, R. J. H., Wade, A. R., & Elliott, C. J. H. (2017). A
822 perspective plus on Parkinson's disease. *Movement Disorders*.

823 Hindle, S., Afsari, F., Stark, M., Adam Middleton, C., Evans, G. J. O., Sweeney, S.
824 T., & Elliott, C. J. H. (2013). Dopaminergic expression of the Parkinsonian gene
825 LRRK2-G2019S leads to non-autonomous visual neurodegeneration,
826 accelerated by increased neural demands for energy. *Human Molecular*

827 *Genetics*, 22(11), 2129–2140. <https://doi.org/10.1093/hmg/ddt061>

828 Hirsh, J., Riemensperger, T., Coulom, H., Ich??, M., Coupar, J., & Birman, S. (2010).
829 Roles of Dopamine in Circadian Rhythmicity and Extreme Light Sensitivity of
830 Circadian Entrainment. *Current Biology*, 20(3), 209–214.
831 <https://doi.org/10.1016/j.cub.2009.11.037>

832 Izenman, A. J. (2008). *Modern Multivariate Statistical Techniques*. New York:
833 Springer-Verlag.

834 Jackson, C. R., Ruan, G.-X., Aseem, F., Abey, J., Gamble, K., Stanwood, G., ...
835 McMahon, D. G. (2012). Retinal Dopamine Mediates Multiple Dimensions of
836 Light-Adapted Vision. *Journal of Neuroscience*, 32(27), 9359–9368.
837 <https://doi.org/10.1523/JNEUROSCI.0711-12.2012>

838 Jolliffe, I. T., & Cadima, J. (2016). Principal component analysis : a review and recent
839 developments Subject Areas : Author for correspondence :

840 Kitada, T., Pisani, A., Porter, D. R., Yamaguchi, H., Tscherter, A., Martella, G., ...
841 Shen, J. (2007). Impaired dopamine release and synaptic plasticity in the
842 striatum of PINK1-deficient mice. *Proc.Natl.Acad.Sci.U.S.A*, 104(0027–8424
843 (Print)), 11441–11446. <https://doi.org/10.1073/pnas.0702717104>

844 Kral, K., & Meinertzhagen, I. a. (1989). Anatomical plasticity of synapses in the
845 lamina of the optic lobe of the fly. *Philosophical Transactions of the Royal*
846 *Society of London. Series B, Biological Sciences*, 323(1214), 155–183.
847 <https://doi.org/10.1098/rstb.1989.0004>

848 Lavara-Culebras, E., Muñoz-Soriano, V., Gómez-Pastor, R., Matallana, E., & Paricio,
849 N. (2010). Effects of pharmacological agents on the lifespan phenotype of
850 *Drosophila* DJ-1 β mutants. *Gene*, 462(1–2), 26–33.
851 <https://doi.org/10.1016/j.gene.2010.04.009>

852 Longo, F., Russo, I., Shimshek, D. R., Greggio, E., & Morari, M. (2014). Genetic and
853 pharmacological evidence that G2019S LRRK2 confers a hyperkinetic
854 phenotype, resistant to motor decline associated with aging. *Neurobiology of*
855 *Disease*, 71, 62–73. <https://doi.org/10.1016/j.nbd.2014.07.013>

856 Martella, G., Madeo, G., Schirinzi, T., Tassone, A., Sciamanna, G., Spadoni, F., ...
857 Bonsi, P. (2011). Altered profile and D2-dopamine receptor modulation of high
858 voltage-activated calcium current in striatal medium spiny neurons from animal
859 models of Parkinson's disease. *Neuroscience*, 177, 240–251.
860 <https://doi.org/10.1016/j.neuroscience.2010.12.057>

861 Matikainen-Ankney, B. A., Kezunovic, N., Mesias, R. E., Tian, Y., Williams, F. M.,
862 Huntley, G. W., & Benson, D. L. (2016). Altered Development of Synapse
863 Structure and Function in Striatum Caused by Parkinson's Disease-Linked
864 LRRK2-G2019S Mutation. *The Journal of Neuroscience : The Official Journal of*
865 *the Society for Neuroscience*, 36(27), 7128–41.
866 <https://doi.org/10.1523/JNEUROSCI.3314-15.2016>

867 Menzies, F. M., Yeniseti, S. C., & Min, K. T. (2005). Roles of Drosophila DJ-1 in
868 survival of dopaminergic neurons and oxidative stress. *Current Biology*, 15(17),
869 1578–1582. <https://doi.org/10.1016/j.cub.2005.07.036>

870 Meulener, M., Whitworth, A. J., Armstrong-Gold, C. E., Rizzu, P., Heutink, P., Wes,
871 P. D., ... Bonini, N. M. (2005). Drosophila DJ-1 mutants are selectively sensitive
872 to environmental toxins associated with Parkinson's disease. *Current Biology*,
873 15(17), 1572–1577. <https://doi.org/10.1016/j.cub.2005.07.064>

874 Michelson, A. (1927). *Studies in Optics*. University of Chicago Press.

875 Mortiboys, H., Furnston, R., Bronstad, G., Aasly, J., Elliott, C., & Bandmann, O.
876 (2015). UDCA exerts beneficial effect on mitochondrial dysfunction in

877 LRRK2(G2019S) carriers and in vivo. *Neurology*, 85(10).
878 <https://doi.org/10.1212/WNL.0000000000001905>.

879 Nassel, D. R., & Elekes, K. (1992). Aminergic neurons in the brain of blowflies and
880 *Drosophila*: dopamine- and tyrosine hydroxylase-immunoreactive neurons and
881 their relationship with putative histaminergic neurons. *Cell Tissue Res.*, 267,
882 147–167.

883 Navarro, J. A., Heßner, S., Yenissetti, S. C., Bayersdorfer, F., Zhang, L., Voigt, A., ...
884 Botella, J. A. (2014). Analysis of dopaminergic neuronal dysfunction in genetic
885 and toxin-induced models of Parkinson's disease in *Drosophila*. *Journal of*
886 *Neurochemistry*, 131(3), 369–382. <https://doi.org/10.1111/jnc.12818>

887 Ng, C.-H., Guan, M. S. H., Koh, C., Ouyang, X., Yu, F., Tan, E.-K., ... Lim, K.-L.
888 (2012). AMP Kinase Activation Mitigates Dopaminergic Dysfunction and
889 Mitochondrial Abnormalities in *Drosophila* Models of Parkinson's Disease.
890 *Journal of Neuroscience*, 32(41), 14311–14317.
891 <https://doi.org/10.1523/JNEUROSCI.0499-12.2012>

892 Norcia, A. M., Appelbaum, L. G., Ales, J. M., Cottreau, B. R., & Rossion, B. (2015).
893 The steady-state visual evoked potential in vision research : A review. *Journal of*
894 *Vision*, 15(6), 1–46. <https://doi.org/10.1167/15.6.4.doi>

895 Ogden, D. (1994). Microelectrode electronics. In D. Ogden (Ed.), *Microelectrode*
896 *Techniques*. Cambridge: Company of Biologists.

897 Oswald, M. C. W., Brooks, P. S., Zwart, M. F., Mukherjee, A., Ryan, J. H., Morarach,
898 K., ... Landgraf, M. (2016). Reactive Oxygen Species Regulate Neuronal
899 Structural Plasticity, 3. <https://doi.org/http://dx.doi.org/10.1101/081968>

900 Park, J., Lee, S. B., Lee, S. B., Kim, Y., Song, S., Kim, S., ... Chung, J. K. (2006).
901 Mitochondrial dysfunction in *Drosophila* PINK1 mutants is complemented by

902 parkin. *Nature*, 441(7097), 1157–1161. <https://doi.org/10.1038/nature04788>

903 Pisani, A., Martella, G., Tscherter, A., Costa, C., Mercuri, N. B., Bernardi, G., ...
904 Calabresi, P. (2006). Enhanced sensitivity of DJ-1-deficient dopaminergic
905 neurons to energy metabolism impairment: Role of Na⁺/K⁺ ATPase.
906 *Neurobiology of Disease*, 23(1), 54–60.
907 <https://doi.org/10.1016/j.nbd.2006.02.001>

908 Ponzo, V., Di Lorenzo, F., Brusa, L., Schirinzi, T., Battistini, S., Ricci, C., ... Koch, G.
909 (2017). Reply Letter to “Does motor cortex plasticity depend on the type of
910 mutation in the LRRK2 gene? *Movement Disorders*, 32(6), 949.

911 Regan, D. (1966). Some characteristics of average steady-state and transient
912 responses evoked by modulated light. *Electroencephalography and Clinical*
913 *Neurophysiology*, 20(3), 238–248.

914 Schapira, A. H. (2008). Mitochondria in the aetiology and pathogenesis of
915 Parkinson’s disease. *The Lancet Neurology*. [https://doi.org/10.1016/S1474-](https://doi.org/10.1016/S1474-4422(07)70327-7)
916 [4422\(07\)70327-7](https://doi.org/10.1016/S1474-4422(07)70327-7)

917 Single, S., Haag, J., & Borst, a. (1997). Dendritic computation of direction selectivity
918 and gain control in visual interneurons. *The Journal of Neuroscience : The*
919 *Official Journal of the Society for Neuroscience*, 17(16), 6023–6030.

920 Sloan, M., Alegre-Abarrategui, J., Potgieter, D., Kaufmann, A. K., Exley, R., Deltheil,
921 T., ... Wade-Martins, R. (2016). LRRK2 BAC transgenic rats develop
922 progressive, L-DOPA-responsive motor impairment, and deficits in dopamine
923 circuit function. *Human Molecular Genetics*, 25(5), 951–963.
924 <https://doi.org/10.1093/hmg/ddv628>

925 Surmeier, D. J., Obeso, J. A., & Halliday, G. M. (2017). Parkinson’s Disease Is Not
926 Simply a Prion Disorder. *Journal of Neuroscience*, 37(41).

927 <https://doi.org/https://doi.org/10.1523/JNEUROSCI.1787-16.2017>

928 Tyler, C. W., Apkarian, P., & Nakayama, K. (1978). Multiple spatial-frequency tuning
929 of electrical responses from human visual cortex. *Experimental Brain Research*,
930 33(3–4), 535–550. <https://doi.org/10.1007/BF00235573>

931 Volta, M., Beccano-Kelly, D. A., Paschall, S. A., Cataldi, S., MacIsaac, S. E.,
932 Kuhlmann, N., ... Milnerwood, A. J. (2017). Initial elevations in glutamate and
933 dopamine neurotransmission decline with age, as does exploratory behavior, in
934 LRRK2 G2019S mice. *Elife*, 20(6). <https://doi.org/10.7554/eLife.28377>

935 Wang, D., Qian, L., Xiong, H., Liu, J., Neckameyer, W. S., Oldham, S., ... Zhang, Z.
936 (2006). Antioxidants protect PINK1-dependent dopaminergic neurons in
937 *Drosophila*. *Proceedings of the National Academy of Sciences of the United*
938 *States of America*, 103(36), 13520–5. <https://doi.org/10.1073/pnas.0604661103>

939 Weil, R. S., Schrag, A. E., Warren, J. D., Crutch, S. J., Lees, A. J., & Morris, H. R.
940 (2016). Visual dysfunction in Parkinson's disease. *Brain*, 139(11), 2827–2843.
941 <https://doi.org/10.1093/brain/aww175>

942 West, R. J. H., Elliott, C. J. H., & Wade, A. R. (2015a). Classification of Parkinson's
943 Disease Genotypes in *Drosophila* Using Spatiotemporal Profiling of Vision.
944 *Scientific Reports*, 5(October), 16933. <https://doi.org/10.1038/srep16933>

945 West, R. J. H., Elliott, C. J. H., & Wade, A. R. (2015b). Classification of Parkinson's
946 Disease Genotypes in *Drosophila* Using Spatiotemporal Profiling of Vision, 5,
947 16933. Retrieved from <http://dx.doi.org/10.1038/srep16933>

948 Witkovsky, P. (2004). Dopamine and retinal function. *Documenta Ophthalmologica*.
949 <https://doi.org/10.1023/B:DOOP.0000019487.88486.0a>

950 Yang, W., Chen, L., Ding, Y., Zhuang, X., & Kang, U. J. (2007). Paraquat induces
951 dopaminergic dysfunction and proteasome impairment in DJ-1-deficient mice.

952 *Human Molecular Genetics*, 16(23), 2900–2910.

953 <https://doi.org/10.1093/hmg/ddm249>

954

955

956

957

958

959

960

961

962

963

964

965

966

967

968

969

970

971

972

973

974

975

976

977

Figure Captions

978 **Figure 1.** Time-domain SSVEP with a stimulus input frequency of 8Hz contains 16
979 'reversals' / second and can be decomposed into a SSVEP response spectrum with
980 peaks at multiples of the input frequency. In A) we present an averaged time-domain
981 SSVEP response from a w^- fly to 99% contrast reversing sine grating over 1000ms,
982 modulating at 8Hz, whilst B) shows Fourier amplitudes decomposed from Fourier
983 transform the 8Hz waveform in A, with peaks occurring at multiples of our input
984 frequency (8Hz, 16Hz, 24Hz, 32Hz, 40Hz). The same is shown in C) and D) for a
985 *PINK1⁵* PD-mutant fly.

986

987 **Figure 2.** Analysis path for Linear Discriminant Analysis (LDA). The raw ERG
988 (electroretinogram) response to 64 different stimuli is collected – here from a control
989 (wild-type) w^- fly and an EOPD (*PINK1*) fly (A). For each stimulus, Fourier analysis
990 is used to measure the response of the fly at the second harmonic ($2f$) (B). Each fly
991 is exposed to 64 stimuli – each with a known contrast and temporal frequency. The
992 heat map (C) represents the amplitude of the second harmonic at each stimulus
993 condition. In this simple case, with just 2 genotypes at one time point, the LDA is
994 applied to the data from both genotypes, and determines the equation that best
995 separates the data into two classes based on the 64 responses. Three outcomes
996 could be envisaged – an optimal separation of the data. Di) a clear line separates the
997 data, or a partial separation (Dii), or no difference (Diii), all the data are mixed). In
998 this portrayal, the graph plots 'X' and 'Y' which will be calculated from the 64 Fourier
999 results by the LDA algorithm. In the more complex dataset explored below, 5
1000 genotypes and 5 ages were sampled, leading to a multi-dimensional 'cloud' of data
1001 which can still be separated by a (more complex) set of linear equations.

1002

1003 **Figure 3.** We use the ERG to obtain accurate SSVEP measurements from both wild-
1004 type and PD *Drosophila* mutants at different contrasts and ages. In A-F we present
1005 exemplar ERG responses at 8Hz obtained from *w⁻* and *PINK1* PD mutants at 1 and
1006 28 days of age, and at 64% and 99% contrast. SSVEP waveform peak amplitude
1007 increases with increasing contrast.

1008

1009 **Figure 4:** EOPD mutants show steeper response amplitudes at 1 day of age. A-E)
1010 Mean response amplitudes from all *Drosophila* genotypes (n=10 for each genotype).
1011 *Drosophila* exhibit visual tuning to temporal frequency and contrast, with peak
1012 sensitivity at 6-8Hz temporal frequency and 99% contrast. Further, the maps appear
1013 to show subtle differences outside of peak regions between 12-36Hz at 1-8%
1014 contrast. Profiles indicate that EOPD mutants have larger response amplitudes at
1015 'peak sensitivity' regions. F) Boxplot of the $2f$ peak response at 99% contrast and
1016 8Hz for each genotype.

1017

1018 **Figure 5.** High contrast (99%) and intermediate temporal frequency combinations (6-
1019 18Hz) conditions exhibit the strongest loading onto the first principal component. The
1020 entire dataset (N=250) is run through the PCA simultaneously to ensure that it is
1021 scaled by the same eigenvalue. Brighter colours represented a higher loading onto
1022 the first PC, whilst darker colours represent a lower loading.

1023

1024 **Figure 6.** One day old EOPD flies show increased SSVEP response amplitudes
1025 when compared to control flies (*w⁻*). Mean PC Score (representing response

1026 amplitude) as a function of age for five *Drosophila* genotypes (n=10 for each
1027 genotype/age group). Error bars show ± 1 SE.

1028

1029 **Figure 7.** All EOPD mutants show perturbations in response amplitudes after
1030 exposure to pulsating light, indicating a decrease in temporal contrast sensitivity
1031 (n=10 per genotype). A-E) Mean response amplitudes from all *Drosophila* genotypes
1032 after 7 days of visual stimulation (each genotype n=10, except *DJ-1 α^{A72}* n=8). Same
1033 scale as Figure 3. F) Boxplot of the *2f* peak response at 99% contrast and 8Hz.

1034

1035 **Figure 8.** Visual loss occurs in all PD mutants after 7 days of exposure to pulsating
1036 light. Mean PC Score of 5 *Drosophila* genotypes after 7 days exposure (each
1037 genotype n=10, except *DJ-1 α^{A72}* n=8).

1038

1039 **Figure 9.** LDA can accurately discriminate between all 25 classes when they are
1040 included in the model. All classifications sit above 4% chance baseline, except for
1041 *PINK1⁵* at 21 days of age.

1042

1043 **Figure 10.** Classification of young flies by genotypic class using data from temporal
1044 contrast response profiles. Mean classification accuracies for N-way LDA of 5
1045 genotypes at 1 day of age (n=10 per genotype). The chance baseline is set at 20%,
1046 with mean classification accuracies between 45.5% and 78.8%.

1047

1048

1049

1050

1051

1052

Statistical Supplements

	w^-	$DJ1-\beta^{\Delta 93}$	$DJ-1\alpha^{\Delta 72}$	$dLRRK^{ex1}$
$PINK1^5$	$p < .001^*$	$p = .724$	$p = .048^*$	$p < .001^*$
w^-	-	$p < .001^*$	$p = .006^*$	$p = .302$
$DJ1-\beta^{\Delta 93}$	-	-	$p = .892$	$p = .083$
$DJ-1\alpha^{\Delta 72}$	-	-	-	$p = .852$

1053

1054 Table 1. Simple Effects Analysis: p -values at 1 day of age

	w^-	$DJ1-\beta^{\Delta 93}$	$DJ-1\alpha^{\Delta 72}$	$dLRRK^{ex1}$
$PINK1^5$	$p = .208$	$p = .158$	$p = .185$	$p = .004^*$
w^-	-	$p = .208$	$p = 1.000$	$p = 1.000$
$DJ1-\beta^{\Delta 93}$	-	-	$p = 1.000$	$p = .940$
$DJ-1\alpha^{\Delta 72}$	-	-	-	$p = .917$

1055

1056 Table 2. Simple Effects Analysis: p -values at 7 days of age

	w^-	$DJ1-\beta^{\Delta 93}$	$DJ-1\alpha^{\Delta 72}$	$dLRRK^{ex1}$
$PINK1^5$	$p = 1.000$	$p = .221$	$p = .042^*$	$p = .019^*$
w^-	-	$p = .064$	$p = .156$	$p = .080$
$DJ1-\beta^{\Delta 93}$	-	-	$p < .001^*$	$p < .001^*$
$DJ-1\alpha^{\Delta 72}$	-	-	-	$p = 1.000$

1057

1058 Table 3. Simple Effects Analysis: p -values at 14 days of age

1059

1060

1061

	w^-	$DJ1-\beta^{\Delta 93}$	$DJ-1\alpha^{\Delta 72}$	$dLRRK^{ex1}$
$PINK1^5$	$p = .897$	$p = .737$	$p = .440$	$p = .862$
w^-	-	$p = .052$	$p = .999$	$p = 1.0$
$DJ1-\beta^{\Delta 93}$	-	-	$p = .006^*$	$p = .042^*$
$DJ-1\alpha^{\Delta 72}$	-	-	-	$p = 1.000$

1062

1063 Table 4. Simple Effects Analysis: p -values at 21 days of age

	w^-	$DJ1-\beta^{\Delta 93}$	$DJ-1\alpha^{\Delta 72}$	$dLRRK^{ex1}$
$PINK1^5$	$p = .515$	$p = 1.000$	$p = .010^*$	$p = .275$
w^-	-	$p = .440$	$p = .753$	$p = 1.000$
$DJ1-\beta^{\Delta 93}$	-	-	$p = .007^*$	$p = .222$
$DJ-1\alpha^{\Delta 72}$	-	-	-	$p = .937$

1064

1065 Table 5. Simple Effects Analysis: p -values at 28 days of age

	7 days	14 days	21 days	28 days
1 day	$p = .001^*$	$p < .001^*$	$p = .05^*$	$p < .001^*$
7 days	-	$p = .811$	$p = 1.000$	$p = 1.000$
14 days	-	-	$p = .372$	$p = .991$
21 days	-	-	-	$p = .951$

1066

1067 Table 6. Simple Effects Analysis: p -values for w^- *Drosophila*

1068

1069

1070

	7 days	14 days	21 days	28 days
1 day	$p = 1.000$	$p = 1.000$	$p = 1.000$	$p = 1.000$
7 days	-	$p = .988$	$p = .938$	$p = .988$
14 days	-	-	$p = 1.000$	$p = 1.000$
21 days	-	-	-	$p = 1.000$

1071

1072 Table 7. Simple Effects Analysis: p -values for $DJ-1\alpha^{\Delta 72}$ *Drosophila*

	7 days	14 days	21 days	28 days
1 day	$p = .988$	$p = .005^*$	$p = .691$	$p = .507$
7 days	-	$p < .001^*$	$p = .178$	$p = .099$
14 days	-	-	$p = .427$	$p = .609$
21 days	-	-	-	$p = 1.000$

1073

1074 Table 8. Simple Effects Analysis: p -values for $DJ1-\beta^{\Delta 93}$ *Drosophila*

	7 days	14 days	21 days	28 days
1 day	$p = 1.000$	$p = 1.000$	$p = .768$	$p = 1.000$
7 days	-	$p = 1.000$	$p = .698$	$p = 1.000$
14 days	-	-	$p = .923$	$p = 1.000$
21 days	-	-	-	$p = .634$

1075

1076 Table 9. Simple Effects Analysis: p -values for $PINK1^5$ *Drosophila*

1077

1078

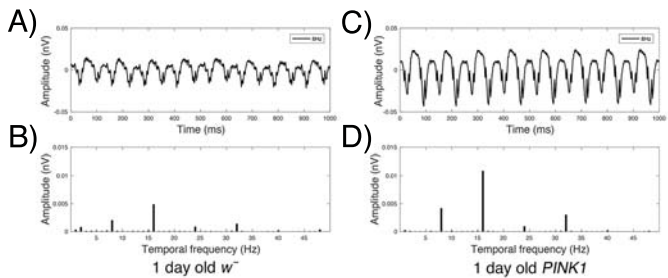
1079

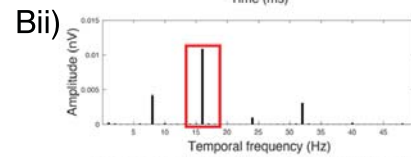
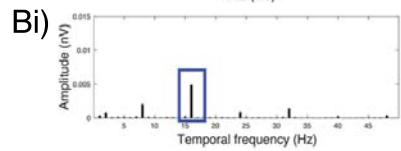
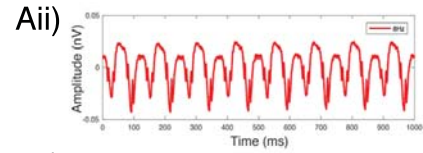
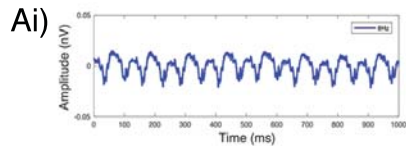
	7 days	14 days	21 days	28 days
1 day	$p = .998$	$p = .997$	$p = .852$	$p = .242$
7 days	-	$p = 1.000$	$p = .999$	$p = .733$
14 days	-	-	$p = .1.000$	$p = .806$
21 days	-	-	-	$p = .993$

1080

1081 Table 10. Simple Effects Analysis: p -values for $dLRRK^{ex1}$ *Drosophila*

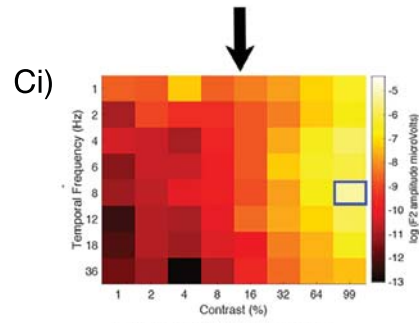
1082



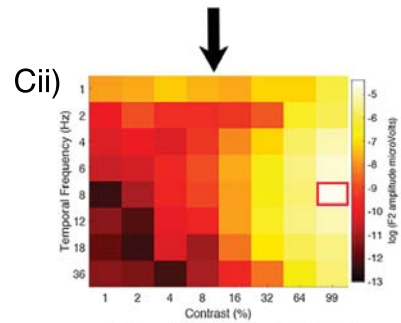


1 day *w* F2 amplitude at 99% contrast, 8Hz

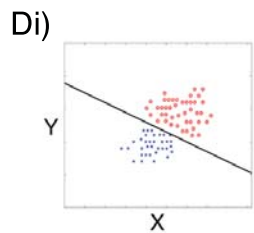
1 day *PINK1* F2 amplitude at 99% contrast, 8Hz



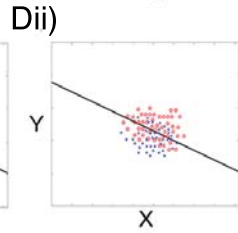
1 day *w* F2 amplitude full profile



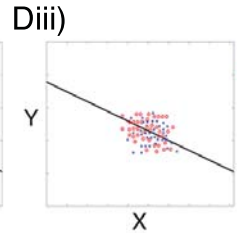
1 day *PINK1* F2 amplitude full profile



High classification accuracy

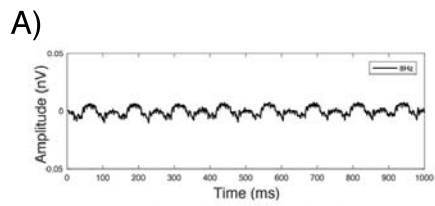


Medium classification accuracy

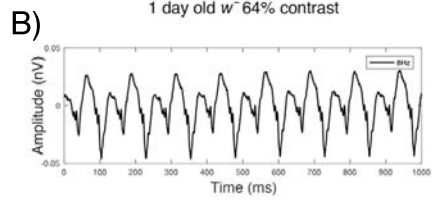


Low classification accuracy

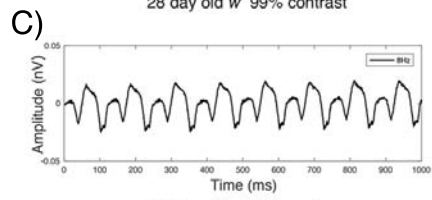
× *w* flies
○ *PINK1* flies



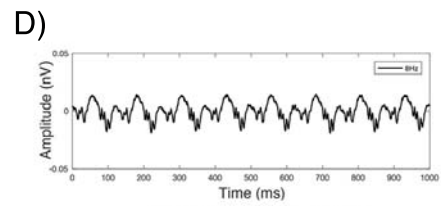
1 day old w⁻ 64% contrast



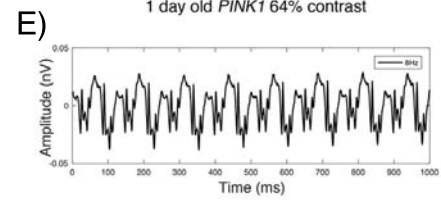
28 day old w⁻ 99% contrast



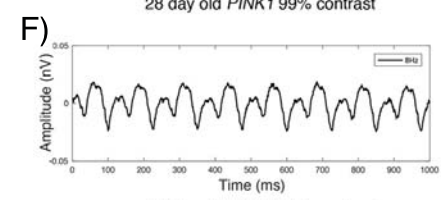
28 day old w⁻ 64% contrast



1 day old *PINK1* 64% contrast



28 day old *PINK1* 99% contrast



28 day old *PINK1* 64% contrast

